

Clonability of printable graphical codes

a machine learning approach

Olga Taran, Slavi Bonev and Slava Voloshynovskiy

Department of Computer Science

May 16, 2019

Outline

State-of-the-art

Machine learning based attacks

Dataset of DataMatrix codes

Regeneration results

Authentication results

Conclusions

State-of-the-art



ID docs



Certificates



Electronics



Banknotes



Luxury objects



Art objects



Packaging

Risks of counterfeiting

- Danger for life
- Market loss
- Damage of brand reputation
- etc.

State-of-the-art



ID docs



Certificates



Electronics



Banknotes



Luxury objects



Art objects



Packaging

- ▶ Special printing Materials or Techniques [WCH⁺13, MGC⁺14]
 - increases the product cost
 - + expensive & difficult for copying

Risks of counterfeiting

- Danger for life
- Market loss
- Damage of brand reputation
- etc.

State-of-the-art



ID docs



Certificates



Electronics



Banknotes



Luxury objects



Art objects



Packaging

- ▶ Special printing Materials or Techniques [WCH⁺13, MGC⁺14]
 - increases the product cost
 - + expensive & difficult for copying
- ▶ Physical Unclonable Functions (PUFs) [VDB⁺12, WW15]
 - verification often requires special equipment
 - + unclonable

Risks of counterfeiting

- Danger for life
- Market loss
- Damage of brand reputation
- etc.

State-of-the-art



ID docs



Certificates



Electronics



Banknotes



Luxury objects



Art objects



Packaging

- ▶ Special printing Materials or Techniques [WCH⁺13, MGC⁺14]
 - increases the product cost
 - + expensive & difficult for copying
- ▶ Physical Unclonable Functions (PUFs) [VDB⁺12, WW15]
 - verification often requires special equipment
 - + unclonable
- ▶ Watermarking [MNI⁺14, XHZT15]
 - anti-copying resistance is questionable

Risks of counterfeiting

- Danger for life
- Market loss
- Damage of brand reputation
- etc.

State-of-the-art



ID docs



Certificates



Electronics



Banknotes



Luxury objects



Art objects



Packaging

Risks of counterfeiting

- Danger for life
- Market loss
- Damage of brand reputation
- etc.

- ▶ Special printing Materials or Techniques [WCH⁺13, MGC⁺14]
 - increases the product cost
 - + expensive & difficult for copying
- ▶ Physical Unclonable Functions (*PUFs*) [VDB⁺12, WW15]
 - verification often requires special equipment
 - + unclonable
- ▶ Watermarking [MNI⁺14, XHZT15]
 - anti-copying resistance is questionable
- ▶ Anti-copying Pattern [Pic04, WB08]
 - + claimed to be **unclonable**

State-of-the-art



ID docs



Certificates



Electronics



Banknotes



Luxury objects



Art objects



Packaging

Risks of counterfeiting

- Danger for life
- Market loss
- Damage of brand reputation
- etc.

- ▶ Special printing Materials or Techniques [WCH⁺13, MGC⁺14]
 - increases the product cost
 - + expensive & difficult for copying
- ▶ Physical Unclonable Functions (PUFs) [VDB⁺12, WW15]
 - verification often requires special equipment
 - + unclonable
- ▶ Watermarking [MNI⁺14, XHZT15]
 - anti-copying resistance is questionable
- ▶ Anti-copying Pattern [Pic04, WB08]
 - ? is it really **unclonable**?

State-of-the-art



Figure 1: Example of traditional 2D codes.

- ▶ Traditional codes are used to encode product info that is used for tracking and tracing

State-of-the-art



Figure 1: Example of traditional 2D codes.

- ▶ Traditional codes are used to encode product info that is used for tracking and tracing
- ▶ However they are clonable

State-of-the-art

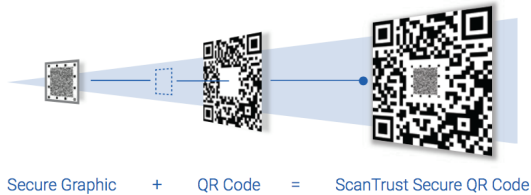


Figure 2: Example of ScanTrust QR code [<https://www.scantrust.com>].

State-of-the-art

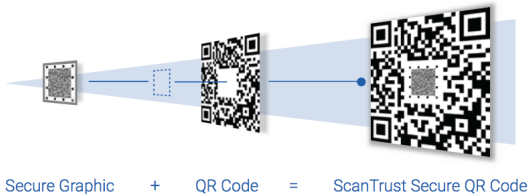


Figure 2: Example of ScanTrust QR code [<https://www.scantrust.com>].

- ▶ These codes referred to as Printable Graphical Codes (PGC) are used to distinguish authentic product from fakes and are claimed to be **unclonable** under **hand-crafted** attacks

State-of-the-art

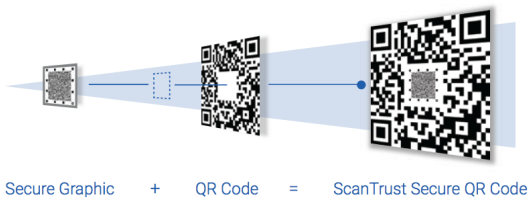


Figure 2: Example of ScanTrust QR code [<https://www.scantrust.com>].

- ▶ These codes referred to as Printable Graphical Codes (PGC) are used to distinguish authentic product from fakes and are claimed to be **unclonable** under **hand-crafted** attacks
- ▶ What about **machine learning based attacks**?

Machine learning based attacks

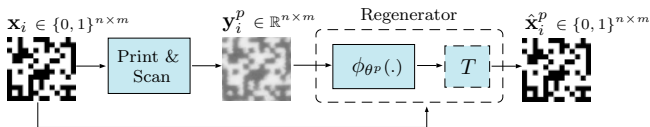


Figure 3: Training procedure based on training samples $\{\mathbf{x}_i, \mathbf{y}_i^p\}_{i=1}^M$ (p - printer type, M - number of training samples and T - thresholding).

Machine learning based attacks

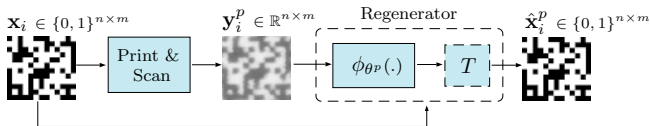


Figure 3: Training procedure based on training samples $\{\mathbf{x}_i, \mathbf{y}_i^p\}_{i=1}^M$ (p - printer type, M - number of training samples and T - thresholding).

Training:

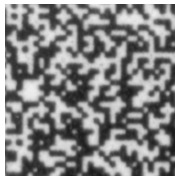
$$\hat{\theta}^p = \arg \min_{\theta^p} \sum_{i=1}^M \mathcal{L}(\mathbf{x}_i, T(\phi_{\theta^p}(\mathbf{y}_i^p))) + \lambda \Upsilon_{\theta^p}(\theta^p) \quad (1)$$

where $\mathcal{L}(\cdot)$ is a loss function, ϕ_{θ^p} is a trained model, θ^p represents the parameters of the trained model for a printer p and $\Upsilon_{\theta^p}(\cdot)$ is a regularizer for the model parameters.

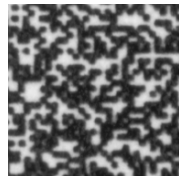
Dataset of *DataMatrix* codes

► Printers:

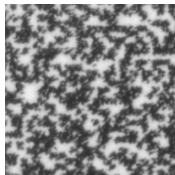
- *Laser*: Samsung Xpress 430 (SA) 600 dpi
- *Laser*: Lexmark CS310 (LX) 1200 dpi
- *Inkjet*: Canon PIXMA iP7200 (CA) 600 dpi
- *Inkjet*: HP OfficeJet Pro 8210 (HP) 1200 dpi



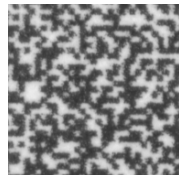
SA



LX



CA



HP

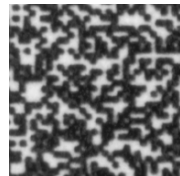
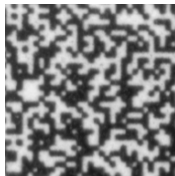
Dataset of *DataMatrix* codes

► Printers:

- *Laser*: Samsung Xpress 430 (SA) 600 dpi
- *Laser*: Lexmark CS310 (LX) 1200 dpi
- *Inkjet*: Canon PIXMA iP7200 (CA) 600 dpi
- *Inkjet*: HP OfficeJet Pro 8210 (HP) 1200 dpi

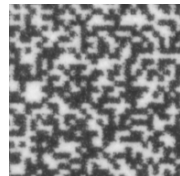
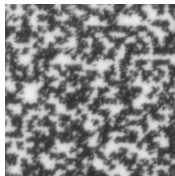
► Scanners:

- Epson V850 Pro at 1200 ppi



SA

LX



CA

HP

Dataset of *DataMatrix* codes

▶ Printers:

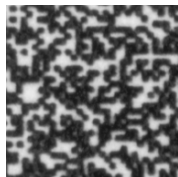
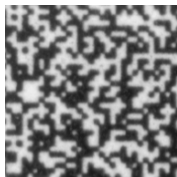
- *Laser*: Samsung Xpress 430 (SA) 600 dpi
- *Laser*: Lexmark CS310 (LX) 1200 dpi
- *Inkjet*: Canon PIXMA iP7200 (CA) 600 dpi
- *Inkjet*: HP OfficeJet Pro 8210 (HP) 1200 dpi

▶ Scanners:

- Epson V850 Pro at 1200 ppi

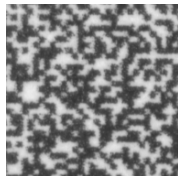
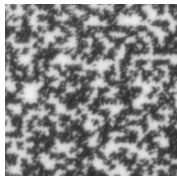
▶ 384 codes of size 384×384 per printer

- training 100 images:
25600 sub-images of size 24×24
- validation 50 images:
12800 sub-images of size 24×24
- test 224 images:
59904 sub-images of size 24×24



SA

LX



CA

HP

Deep FC regenerator

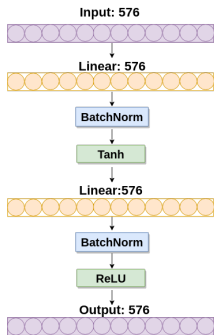


Figure 4: FC 2 layers.

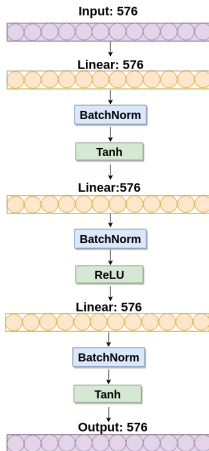


Figure 5: FC 3 layers.

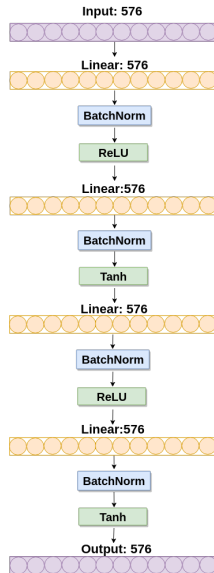


Figure 6: FC 4 layers.

Deep BN regenerator

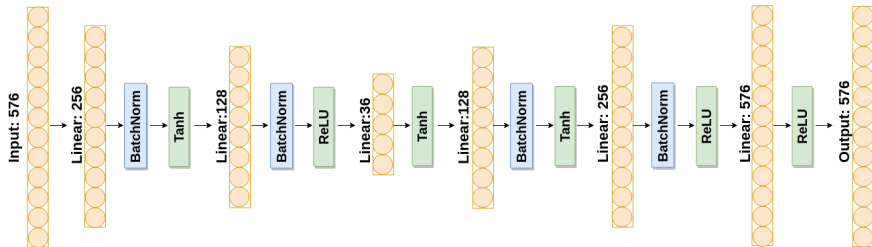


Figure 7: Deep BN regenerator architecture.

Regeneration metrics

- ▶ Hamming distance: $\mathbf{x} \in \{0, 1\}^{n \times m}$, $\mathbf{y}^p \in \mathbb{R}^{n \times m}$, $T_{\vartheta^p}(\cdot)$ - binarization function: ("hard" coding)

$$d(\mathbf{x}, \mathbf{y}^p) = \frac{1}{n \cdot m} \sum_{j=1}^{n \cdot m} \mathbf{x}(j) \oplus T_{\vartheta^p}(\mathbf{y}^p(j)) \quad (2)$$

Regeneration metrics

- ▶ Hamming distance: $\mathbf{x} \in \{0, 1\}^{n \times m}$, $\mathbf{y}^p \in \mathbb{R}^{n \times m}$, $T_{\vartheta}(\cdot)$ - binarization function: ("hard" coding)

$$d(\mathbf{x}, \mathbf{y}^p) = \frac{1}{n \cdot m} \sum_{j=1}^{n \cdot m} \mathbf{x}(j) \oplus T_{\vartheta}(\mathbf{y}^p(j)) \quad (2)$$

- ▶ Pearson correlation [PHMHSB13]: $\mathbf{x} \in \{0, 1\}^{n \times m}$, $\mathbf{y}^p \in \mathbb{R}^{n \times m}$: ("soft" coding)

$$\rho(\mathbf{x}, \mathbf{y}^p) = \frac{\text{cov}(\mathbf{x}, \mathbf{y}^p)}{\sigma_{\mathbf{x}} \sigma_{\mathbf{y}^p}} \quad (3)$$

Regeneration results

| Method | SA | LX | HP | CA |
|------------------------------------|--------------|--------------|--------------|--------------|
| <i>Pearson correlation</i> | | | | |
| <i>Thr</i> | 0.774 | 0.766 | 0.742 | 0.704 |
| <i>FC 2</i> | 0.995 | 0.994 | 0.982 | 0.981 |
| <i>FC 3</i> | 0.994 | 0.994 | 0.982 | 0.983 |
| <i>FC 4</i> | 0.994 | 0.995 | 0.981 | 0.982 |
| <i>BN</i> | 0.996 | 0.996 | 0.986 | 0.984 |
| <i>normalized Hamming distance</i> | | | | |
| <i>Thr</i> | 11 | 12 | 13 | 15 |
| <i>FC 2</i> | 0.22 | 0.24 | 0.93 | 0.98 |
| <i>FC 3</i> | 0.23 | 0.24 | 0.90 | 0.85 |
| <i>FC 4</i> | 0.24 | 0.23 | 0.95 | 0.90 |
| <i>BN</i> | 0.21 | 0.22 | 0.69 | 0.76 |

Table 1: Regeneration results with respect to original codes.

Results visualisation










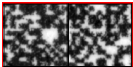



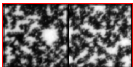


| | Printer | Original | Scanned original | Reconstructed (<i>BN</i>) | Difference |
|-----------------|---------|---|---|--|---|
| Laser printers | SA |  |  |  |  |
| | LX |  |  |  |  |
| Inkjet printers | HP |  |  |  |  |
| | CA |  |  |  |  |

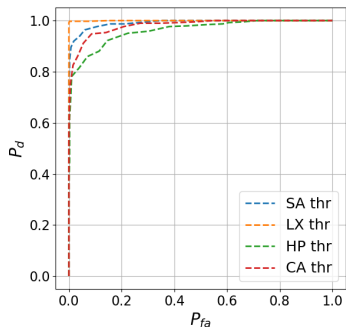
Table 2: Examples of attacks against PGC: two samples of scanned codes, the estimates produced by *BN* model and the difference between the original and attacked codes.

Authentication metrics

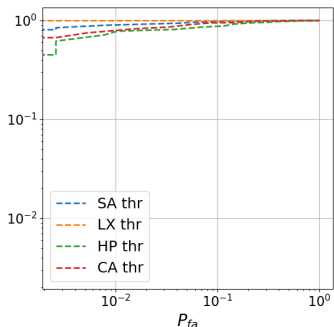
$$\begin{aligned} P_d &= \Pr\{\alpha \cdot d(\mathbf{x}_i, \mathbf{y}_i^p) \leq \gamma | \mathcal{H}_0\} \\ P_{fa} &= \Pr\{\alpha \cdot d(\mathbf{x}_i, \mathbf{y}_i^p) < \gamma | \mathcal{H}_1\}, \end{aligned} \tag{4}$$

where γ is the threshold, $d(\cdot)$ is a similarity measure between the original and printed codes, \mathcal{H}_0 corresponds to the hypothesis that \mathbf{y}_i^p is an authentic code and \mathcal{H}_1 is the hypothesis that \mathbf{y}_i^p is a fake (cloned) code, α equals to -1 for the *Pearson correlation* and to 1 for *Hamming distance*.

Authentication results



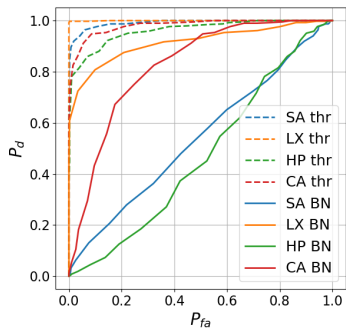
(a) Hamming distance



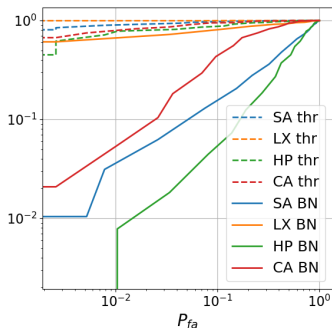
(b) Hamming distance: log scale

Figure 8: The ROC curves for *Hamming distance* between the original and fake printed codes estimated via *Thr* methods. P_d denotes the probability of the correct detection and P_{fa} is the probability of false acceptance.

Authentication results



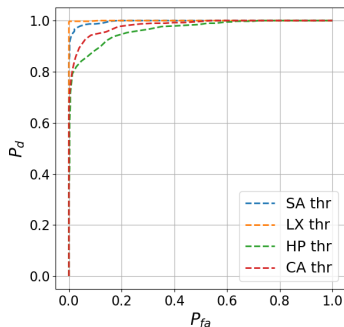
(a) Hamming distance



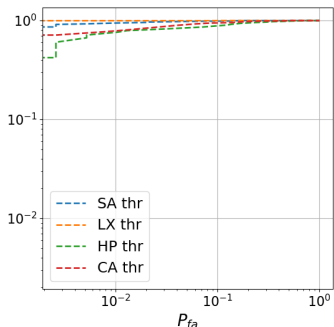
(b) Hamming distance: log scale

Figure 9: The ROC curves for *Hamming distance* between the original and fake printed codes estimated via *BN* and *Thr* methods. P_d denotes the probability of the correct detection and P_{fa} is the probability of false acceptance.

Authentication results



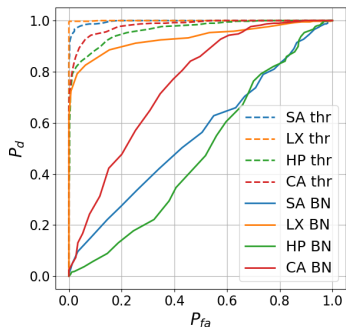
(a) Pearson correlation



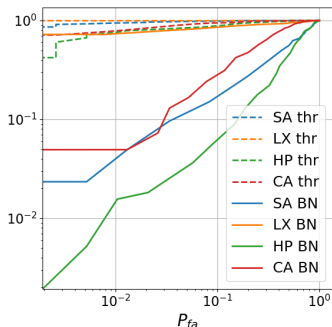
(b) Pearson correlation: log scale

Figure 10: The ROC curves for *Pearson correlation* between the original and fake printed codes estimated via *Thr* methods. P_d denotes the probability of the correct detection and P_{fa} is the probability of false acceptance.

Authentication results



(a) Pearson correlation



(b) Pearson correlation: log scale

Figure 11: The ROC curves for *Pearson correlation* between the original and fake printed codes estimated via *BN* and *Thr* methods. P_d denotes the probability of the correct detection and P_{fa} is the probability of false acceptance.

Conclusions

- ▶ we investigated the clonability of generic printable graphical codes using machine learning based attacks
- ▶ we examined the proposed framework on real printed codes reproduced with 4 printers
- ▶ we demonstrated a possibility of sufficiently accurate cloning of the PGC from their printed counterparts
- ▶ this should serve as a warning that more research are needed on the colonability of PGC

web-page:

<http://sip.unige.ch/projects/snf-it-dis/publications/icassp-2019>




GitHub:

<https://github.com/taran0/clonability-of-printable-graphical-codes>





Dataset:

<http://sip.unige.ch/projects/snf-it-dis/datasets/dp0e/>



References I

-  Xavier Marguerettaz, Frédéric Gremaud, Aurélien Commeureuc, Vickie Aboutanos, Thomas Tiller, and Olivier Rozumek, *Identification and authentication using liquid crystal material markings*, June 3 2014, US Patent 8,740,088.
-  Takeru Maehara, Kentaro Nakai, Ryo Ikeda, Koutaro Taniguchi, and Satoshi Ono, *Watermark design of two-dimensional barcodes on mobile phone display by evolutionary multi-objective optimization*, 2014 Joint 7th International Conference on Soft Computing and Intelligent Systems (SCIS) and 15th International Symposium on Advanced Intelligent Systems (ISIS), IEEE, 2014, pp. 149–154.
-  Anh Thu Phan Ho, Bao An Mai Hoang, Wadih Sawaya, and Patrick Bas, *Document authentication using graphical codes: impacts of the channel model*, Proceedings of the first ACM workshop on Information hiding and multimedia security, ACM, 2013, pp. 87–94.

References II

-  Justin Picard, *Digital authentication with copy-detection patterns*, Optical Security and Counterfeit Deterrence Techniques V, vol. 5310, International Society for Optics and Photonics, 2004, pp. 176–184.
-  Sviatoslav Voloshynovskiy, Maurits Diephuis, Fokko Beekhof, Oleksiy Koval, and Bruno Keel, *Towards reproducible results in authentication based on physical non-cloneable functions: The forensic authentication microstructure optical set (famos)*, 2012 IEEE International Workshop on Information Forensics and Security (WIFS), IEEE, 2012, pp. 43–48.
-  Bernhard Wirnitzer and Slavtcho Bonev, *Matrix print data storage and method for encoding the data*, August 21 2008, US Patent App. 11/572,591.
-  Hsi-Chun Wang, Ya-Wen Cheng, Wan-Chi Huang, Chia-Long Chang, and Shih-Yun Lu, *Using modified digital halftoning technique to design invisible 2d barcode by infrared detection*, Intelligent Technologies and Engineering Systems, Springer, 2013, pp. 179–186.

References III

-  Chau-Wai Wong and Min Wu, *A study on puf characteristics for counterfeit detection*, 2015 IEEE International Conference on Image Processing (ICIP), IEEE, 2015, pp. 1643–1647.
-  Rongsheng Xie, Chaoqun Hong, Shunzhi Zhu, and Dapeng Tao, *Anti-counterfeiting digital watermarking algorithm for printed qr barcode*, Neurocomputing **167** (2015), 625–635.